Energy Advances

ROYAL SOCIETY OF CHEMISTRY

PAPER

View Article Online
View Journal | View Issue

Cite this: *Energy Adv.*, 2022, 1, 1028

Flexible "polymer-in-ceramic" composite solid electrolyte PI–$PEO_{0.2}$–PDA@$LATP_{0.8}$ and its ionic conductivity†

Lei He,[a] Jian-Hua Cao,[a] Ya-Kun Wang[b] and Da-Yong Wu *[a]

Increasing the proportion of inorganic electrolytes in organic–inorganic composite electrolytes can significantly improve the ionic conductivity of composite electrolytes. However, this method is confronted with some problems, such as the uneven dispersion of inorganic electrolytes and the aggregation of nanoparticles, which results in a worse performance of the electrolytes' interface. In this study, we had the dopamine hydrochloride molecules self-polymerized on the surface of inorganic ionic conductor lithium titanium aluminum phosphate (LATP) particles to obtain PDA-coated LATP nanoparticles. Then, the coated LATP particles were composited with PEO at a ratio of 80 : 20, with the LATP's evenly dispersed in the PEO, and no aggregation happened. On adding a small amount of electrolyte (5 μL cm^{-2}, 1 M Li TFSI), the ionic conductivity of the electrospun PI-loaded $PEO_{0.2}$–PDA@$LATP_{0.8}$ flexible composite solid electrolyte reached 2.07×10^{-4} at 30 °C and 2.05×10^{-3} S cm^{-1} at 80 °C. NCM811‖Li batteries assembled with this electrolyte had an initial discharge capacity of 178.0 mA h g^{-1} at 30 °C, and still remained at 172.1 mA h g^{-1} (96.7%) after 200 cycles. The research shows that there are three main conduction pathways of Li^+ in this electrolyte: through the segments of the polymer chains, through the interface between the polymer and inorganic ionic conductor, and through the passage composed of a continuous inorganic ionic conductor. Further results show that the coating of LATP by PDA does not block the transmission of Li^+ both inside the crystal and at the crystal interface of LATP.

Received 23rd August 2022,
Accepted 24th October 2022

DOI: 10.1039/d2ya00224h

rsc.li/energy-advances

1 Introduction

The prospect that a solid electrolyte could replace a traditional separator and all or most of the liquid electrolyte would endow high-energy density batteries with safety characteristics.[1,2] Inorganic electrolytes have a high ionic conductivity (10^{-4}–10^{-2} S cm^{-1}), high thermal stability and mechanical strength, but poor processability; while polymer electrolytes, though flexible and easy to process, exhibit a low conductivity and mechanical modulus. organic–inorganic composite electrolytes not only combine the advantages of inorganic ionic conductors and polymer electrolytes, but also avoid the defects of a single component, and are capable of providing a superior ionic conductivity and mechanical strength, along with easy-to-manufacture feature.[3,4] The key to constructing excellent organic–inorganic composite electrolytes is to obtain a high ionic conductivity, inhibit lithium dendrite growth and reduce interface resistance while balancing the mechanical strength and flexibility of materials.[5]

Common inorganic fast lithium–ion conductors include $Li_{1.4}Al_{0.4}Ti_{1.6}(PO_4)_3$ (LATP),[6] $Li_{10}GeP_2S_{12}$ (LGPS),[7] $Li_7La_3Zr_2O_{12}$ (LLZO)[8] and $Li_{0.35}La_{0.55}TiO_3$ (LLTO) *etc.*,[9] which are usually composited with polymer electrolytes in lower proportions. Increasing the proportion of inorganic ionic conductors will improve the ionic conductivity and thermal stability of organic–inorganic composite solid electrolytes. For example, Chen *et al.* successfully prepared a so-called "polymer in ceramic" composite solid electrolyte containing 80 wt% LLZTO and 20 wt% PEO with a high mechanical strength and safety.[10] However, the nanoscale inorganic particles tend to aggregate, which increases the interface resistance between the polymer and the particles and thereby hinders the rapid diffusion of lithium ions.[11] Therefore, it is particularly important to solve the problem of agglomeration of a high proportion of inorganic nanoparticles in an organic matrix.[12] The conduction pathways

[a] *Technical Institute of Physics and Chemistry, Chinese Academy of Sciences, 29 Zhong-guan-cun East Road, Haidian District, Beijing 100190, P. R. China. E-mail: dayongwu@mail.ipc.ac.cn*
[b] *School of Foreign Studies, China University of Political Science and Law, 27 Fuxue Road, Changping District, Beijing 102249, P. R. China*

† Electronic supplementary information (ESI) available: Images before and after dopamine polymerization, contact angles of PEO solution on LATP and PDA@LATP sheet surface, and p of PI-$PEO_{0.2}$-PDA@$LATP_{0.8}$ electrolyte membrane before and after bending. See DOI: https://doi.org/10.1039/d2ya00224h

of lithium ion in composite solid electrolytes include a ceramic crystal phase, an organic/inorganic interface and a PEO chain segment. There are three possible reasons for the improvement of ion conductivity of composite electrolytes, including reducing the crystallinity of the polymer electrolytes,[13] changing the binding state of the lithium ions with polymers,[14] and enhancing the transmission of the lithium ions at the polymer/inorganic particle interface.[15] In some cases, adding inactive inorganic nanoparticles, such as SiO_2 and Al_2O_3, to polymer electrolytes can also reduce their crystallinity and therefore improve the ionic conductivity. In a previous study, we filled an electrospun PI film with a composite of LATP nanoparticles and PEO (15 : 85) to construct a flexible composite solid electrolyte, and achieved a good battery application performance.[16] Meanwhile, we found that when the content of LATP was higher than 15 wt%, the particles were easy to aggregate, the morphology of composite electrolyte was degraded, and the ionic conductivity dropped. Therefore, in this study, we used dopamine[17] with a good adhesion on the solid surface to coat LATP nanoparticles so as to improve the doping proportion of LATP in the PEO by way of reducing their surface energy. Afterwards, we loaded LATP–PEO onto an electrospun PI film to make an organic–inorganic composite solid electrolyte, followed by investigating its battery application performance and lithium ion conduction mechanism.

2 Results and discussion

2.1 Self-polymerization of dopamine on LATP particle surface

Dopamine molecules contain catechol functional groups, which will undergo oxidative self-polymerization under weak alkaline conditions containing oxygen and water, resulting in a series of oligomers with different molecular weights. Due to the synergistic effect of covalent and non-covalent bonds between them, dopamine, dopamine oxide, dopamine oligomers and polymers will spontaneously assemble in solution to form assemblies with different structures, called polydopamines. This self-polymerization process is well illustrated in Scheme 1. PDA's polymerization rate is related to the oxygen concentration and pH value of the solution. We used an open reactor, maintained the pH value of the reaction medium at 8.5 with Tris–HCl buffer, and mechanically stirred (300 rpm) to make the reaction happen. When dopamine started to polymerize and the solution changed from colorless to dark brown, LATP particles were added. PDA was deposited on the surface of the LATP particles while polymerizing. LATP particles are white in color, while PDA coated LATP particles are light brown (Fig. S1, ESI†).

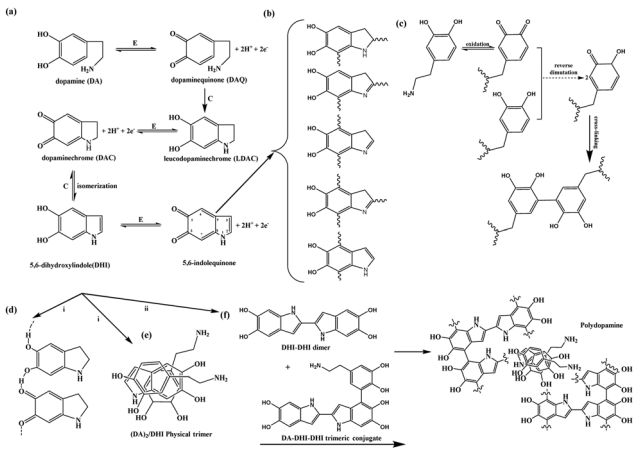

Scheme 1 Self-polymerization of dopamine.[17]

2.2 Morphology of PDA@LATP particles

The TEM morphology of dopamine-coated LATP particles is shown in Fig. 1a, with the particle size between 500 and 600 nm. Additionally, the striped lattice pattern on the LATP particles and the dense amorphous polydopamine coating on the surface of the particles can be clearly observed in the high-resolution TEM image (Fig. 1b). The elemental distribution mappings of PDA@LATP particles are shown in Fig. 1d–i. The Ti, P, O, and Al elements come from the LATP particle, while the N, C and O elements belong to PDA. Moreover, the distribution shape of the C and N elements match the elemental distribution of the LATP particle. It is demonstrated that PDA was successfully coated onto the LATP particles.

2.3 Effect of PDA coating on the dispersion of LATP in PEO

In our previous study,[16] we found that when the ratio of LATP to PEO was greater than 15 : 85, LATP particles agglomerated in the PEO. Therefore, in this study, we increased the ratio of LATP to PEO to 80 : 20, and meanwhile tried to inhibit the agglomeration of LATP particles by coating PDA. When observing the PI–$PEO_{0.8}$–$LATP_{0.2}$ electrolyte membrane through SEM, we found that the LATP particles in the sample were

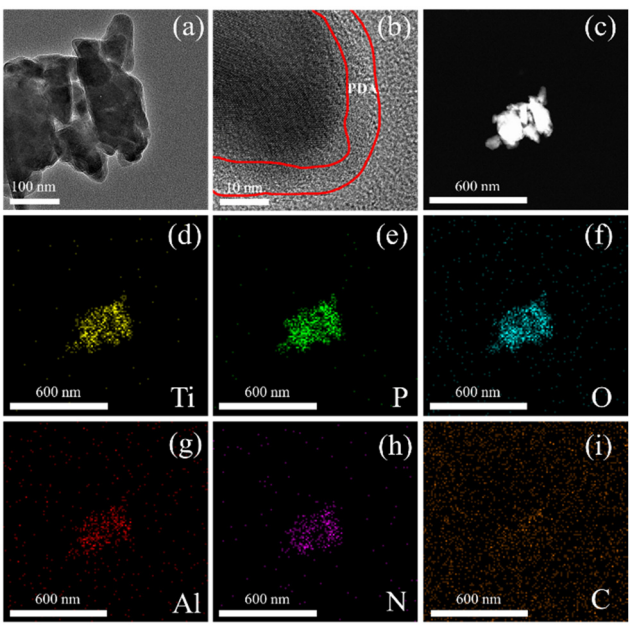

Fig. 1 TEM images of PDA@LATP particles at different magnifications (a–c); EDS mapping of (d) Ti; I P; (f) O; (g) Al; (h) N; (i) C.

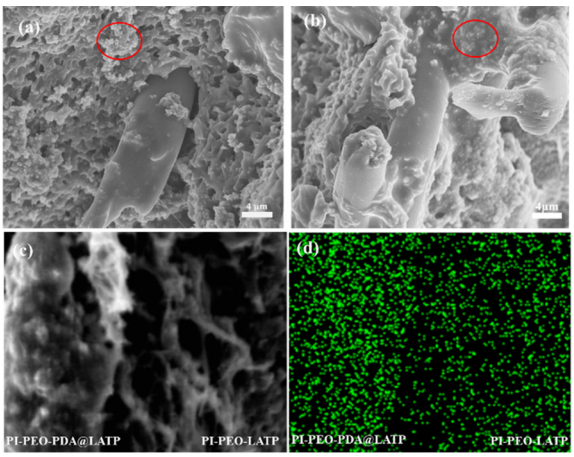

Fig. 2 (a) Cross-section SEM image of PI–$PEO_{0.8}$–$LATP_{0.2}$ film; (b) cross section SEM image of PI–$PEO_{0.2}$–PDA@$LATP_{0.8}$ film; (c) SEM image of PI–$PEO_{0.2}$–PDA@$LATP_{0.8}$|PI–$PEO_{0.8}$–$LATP_{0.2}$; (d) Ti element mapping of PI–$PEO_{0.2}$–PDA@$LATP_{0.8}$ | PI–$PEO_{0.8}$–$LATP_{0.2}$.

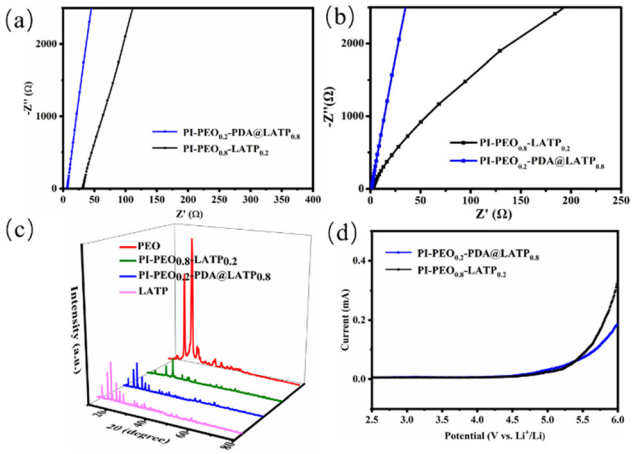

Fig. 3 Nyquist plots of PI–$PEO_{0.8}$–$LATP_{0.2}$ and PI–$PEO_{0.2}$–PDA@$LATP_{0.8}$ at (a) 30 °C and (b) 80 °C; (c) XRD patterns of PEO, PI–$PEO_{0.8}$–$LATP_{0.2}$, PI–$PEO_{0.2}$–PDA@$LATP_{0.8}$ and LATP (d) LSV curves of PI–$PEO_{0.8}$–$LATP_{0.2}$ and PI–$PEO_{0.2}$–PDA@$LATP_{0.8}$ solid-state electrolytes.

agglomerated (Fig. 2a, red cycle). Compared with the PI–$PEO_{0.8}$–$LATP_{0.2}$ electrolyte membrane, the surface of the PI–$PEO_{0.2}$–PDA@$LATP_{0.8}$ electrolyte membrane is smoother and denser.

SEM images show that the LATP particles coated with PDA were evenly dispersed in the PEO matrix, with no aggregation observed (Fig. 2b). Furthermore, we stuck PI–$PEO_{0.2}$–PDA@$LATP_{0.8}$ together with PI–$PEO_{0.8}$–$LATP_{0.2}$, and tested the content of Ti on the cross sections of the two electrolyte membranes using EDS energy spectrum detection. The detection shows that the signal intensity of the Ti element in PI–$PEO_{0.2}$–PDA@$LATP_{0.8}$ on the left is significantly higher than that in PI–$PEO_{0.8}$–$LATP_{0.2}$ on the right, demonstrating that LATP is evenly distributed in PEO.

2.4 The significance of inorganic ionic conductors on the properties of composite electrolytes

The ionic conductivity is a key parameter to evaluate the performance of a solid electrolyte. We measured the ionic conductivity of the solid electrolyte at 30 and 80 °C by an AC impedance method, as shown in Fig. 3a and b. The AC impedance spectrum takes on an approximately straight line in the high frequency region, indicating the fact that lithium ions are carriers, and the ionic conductivity is the total conductivity. The ionic conductivity of PI–$PEO_{0.2}$–PDA@$LATP_{0.8}$ is calculated according to a formula[16] and is 2.07×10^{-4} S cm^{-1} at 30 °C and 2.05×10^{-3} S cm^{-1} at 80 °C; while the corresponding data for PI–$PEO_{0.8}$–$LATP_{0.2}$ is 5.01×10^{-5} S cm^{-1} and 9.31×10^{-4} S cm^{-1}, respectively. This clearly proves that organic–inorganic composite electrolytes with a high content of inorganic ionic conductors have a superior ionic conductivity. Hence, efforts to increase the content of inorganic ionic conductors are of great significance.

Adding a ceramic filler can reduce the crystallinity of PEO, thereby improving its ionic conductivity.[9] We analyzed the phase characteristics of PEO, $PEO_{0.8}$–$LATP_{0.2}$, $PEO_{0.2}$–PDA@$LATP_{0.8}$ and LATP, and found from the XRD pattern of $PEO_{0.8}$–$LATP_{0.2}$ that the characteristic peak of PEO (2θ = 23.2°) is significantly weakened; while from the spectrum of $PEO_{0.2}$–PDA@$LATP_{0.8}$ and that of LATP as well (Fig. 3c), no peak of PEO is observed, indicating LATP, which accounts for 80% of the mass in the complex, hinders the crystallization of PEO.

In the LSV test, we found that both PI–$PEO_{0.8}$–$LATP_{0.2}$ and PI–$PEO_{0.2}$–PDA@$LATP_{0.8}$ began to generate a redox current after 5 V (Fig. 3d). Their electrochemical stability windows are 5.1 and 5.2 V, respectively, indicating that PI-PEO-LATP is an electrochemically stable system with a high voltage resistance.

The coating of LATP particles with PDA not only can improve the uniform dispersion of LATP particles in PEO, thus increasing the content of LATP in the PI-PEO-LATP composite electrolyte, but also improve the flexibility of the PI-PEO-LATP composite electrolyte. A bending-stretching of the electrolyte membrane was carried out with a self-made machine. The optical photos of the membrane before and after 600 times of bending (Fig. S3, ESI†) show that the appearance of the membrane did not changed even slightly after bending. At the same time, the lithium ion conductivity of the membrane before and after bending was 2.07×10^{-4} S cm^{-1} and 1.85×10^{-4} S cm^{-1}, respectively (at 30 °C). No significant attenuation of lithium ion conductivity was found.

2.5 Battery application performance

We assembled a 2032 battery, using NCM811 as the positive electrode, a lithium metal sheet as the negative electrode, and PI–$PEO_{0.8}$–$LATP_{0.2}$ and PI–$PEO_{0.2}$–PDA@$LATP_{0.8}$ as electrolytes. In order to improve the interfacial affinity between the electrode and electrolyte, we added a small amount of electrolyte (1 M LiTFSI in DMC : EC = 1 : 1, 5 μL cm^{-2}) between the negative electrode and the electrolyte. The cycle performance of the battery was tested at 30 °C and 0.2C. The results are shown in Fig. 4a. The first discharge capacity of the battery with the PI–$PEO_{0.2}$–PDA@$LATP_{0.8}$ electrolyte is 178.0 mA h g^{-1}, and the

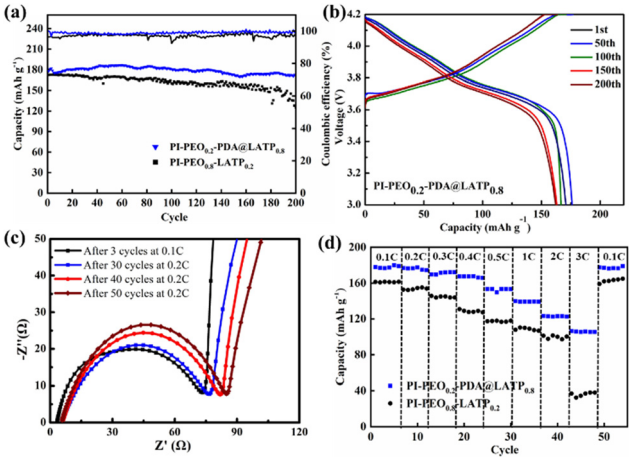

Fig. 4 Performance of the batteries with different electrolytes at 30 °C (a) cycling performance; (b) charge and discharge profiles and (c) Nyquist plots of NCM811/PI–$PEO_{0.2}$–PDA@$LATP_{0.8}$/Li cell under different cycle numbers; (d) rate performance.

remaining capacity after 200 cycles is 172.1 mA h g^{-1} (96.7%), and the coulomb efficiency is close to 100%; in contrast, the discharge capacity of the battery with the PI–$PEO_{0.8}$–$LATP_{0.2}$ electrolyte after 200 cycles is only 124.9 mA h g^{-1}. This resulted from the aggregation and uneven dispersion of LATP particles, which affects the performance of the battery. Fig. 4b is a typical charge and discharge curve of the NCM811‖Li batteries with the PI–$PEO_{0.2}$–PDA@$LATP_{0.8}$ electrolyte. The discharge capacity of the battery decayed slowly with the increase in cycling times.

We tested the interface resistance of NCM811‖Li cells with the PI–$PEO_{0.8}$–$LATP_{0.2}$ electrolyte after the 3rd, 30th, 40th and 50th cycles. The results are shown in Fig. 5c. The battery interface resistances after three cycles are 70.07 Ω. After 30, 40 and 50 cycles at 0.2C, the interface resistances increased to 70.67, 75.70 and 79.12 Ω, respectively.

The discharge capacity of batteries using the PI–$PEO_{0.2}$–PDA@$LATP_{0.8}$ electrolyte in the test of rate performance are 179.5, 177.8, 172.1, 167.3, 153.5, 139.2, 122.7 and 105.5 mA h g^{-1}, respectively, at 0.1, 0.2, 0.3, 0.4, 0.5, 1, 2 and 3C, significantly higher than the values of the PI–$PEO_{0.8}$–$LATP_{0.2}$ electrolyte batteries, *i.e.*, 161.2 and 153.5, 144.6, 128.6, 117.4, 108.6, 99.6 and 36.2 mA h g^{-1}, respectively.

After cycling for 60 cycles at 0.2C and 30 °C, we disassembled the batteries assembled with different electrolytes and found differences in the morphology of the lithium anodes. As shown in Fig. 5, batteries using the PI–$PEO_{0.2}$–PDA@$LATP_{0.8}$ composite electrolyte had a smoother lithium anode surface and the thickness of the deposition layer was thinner. This is mainly due to the high ionic conductivity of the electrolyte. As mentioned above, the ionic conductivity of the PI–$PEO_{0.2}$–PDA@$LATP_{0.8}$ electrolyte is almost an order of magnitude higher than that of the PI–$PEO_{0.8}$–$LATP_{0.2}$ electrolyte at 30 °C. Moreover, the transport mechanism of the lithium ion in the polymer electrolyte affects the morphology of the lithium metal anode. Xiong *et al.* carried out a series of theoretical and experimental studies on the electrodeposition of the lithium metal anode by using an electro-chemo-mechanical mode and proved the above statement.[20–22]

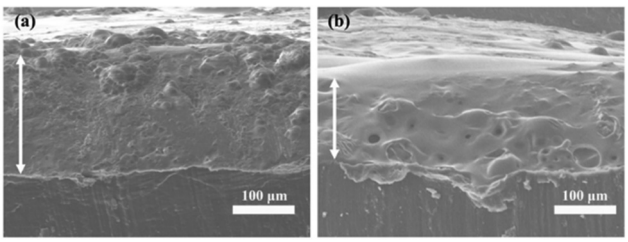

Fig. 5 SEM cross-section images of the lithium anode in contact with (a) the PI–$PEO_{0.8}$–$LATP_{0.2}$ electrolyte; (b) the PI–$PEO_{0.2}$–PDA@$LATP_{0.8}$ electrolyte.

2.6 Enhancement of LATP interface performance by PDA coating

As shown in the results of the battery performance tests, the performance of the PI–$PEO_{0.2}$–PDA@$LATP_{0.8}$ electrolyte is significantly superior to that of PI–$PEO_{0.8}$–$LATP_{0.2}$. The possible reason is that the PI–$PEO_{0.2}$–PDA@$LATP_{0.8}$ electrolyte has a higher ionic conductivity and better compatibility with PEO. To compare the compatibility between different solid electrolytes and PEO, we pressed LATP and PDA@LATP powder in thin sheets, and measured the contact angles of 5a % PEO acetonitrile solution on their surfaces. The results were 115.4° and 75.8°, respectively (Fig. S2, ESI†). The contact angle of PEO and PDA@LATP is smaller, meaning that the two can produce a compatible interface after being mixed. PDA coating reduces the surface energy of the LATP nanoparticles and improves the interface affinity between inorganic ionic conductors and PEO.[18,19]

2.7 Transport mechanism of lithium ion in PI–PEO–LATP solid electrolyte

It has been reported that there are three possible lithium ion transmission pathways in polymer composite electrolytes containing inorganic ion conductors, including conduction through polymer chain segments, conduction through the interface between the polymer and inorganic ion conductors, and conduction through the pathway composed of continuous inorganic ion conductors.[15]

In this work, we coated LATP particles with PDA to improve the dispersion of LATP in PEO. Then, a question arises: does PDA coating block the conduction of Li^+ inside inorganic ionic conductors and between particles? To get the answer, we prepared a PI–$PEO_{0.2}$–PDA@$(Al_2O_3)_{0.8}$ electrolyte with the same amount of inactive material Al_2O_3 nanoparticles instead of LATP, and carried out a control experiment. Nyquist plots of several composite solid electrolytes are shown in Fig. 6.

The test results show that the ionic conductivities of PI–$PEO_{0.2}$–PDA@$(Al_2O_3)_{0.8}$ at 30 and 80 °C are 1.03×10^{-5} and 5.24×10^{-4} S cm^{-1}, respectively, less than both that of PI–$PEO_{0.2}$–PDA@$LATP_{0.8}$, *i.e.*, 2.07×10^{-4} and 2.05×10^{-3} S cm^{-1}, and that of PI–$PEO_{0.8}$–$LATP_{0.2}$, 5.01×10^{-5} and 9.31×10^{-4} S cm^{-1} (Table 1) as well. The effect of adding ceramic particles at low

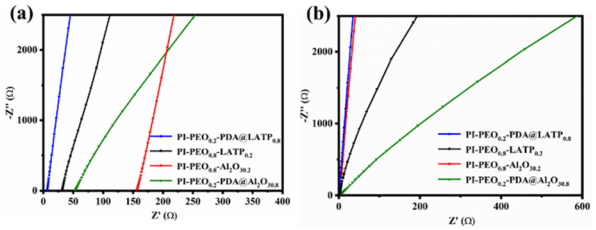

Fig. 6 Nyquist plots of several composite solid electrolytes at (a) 30 °C; (b) 80 °C.

Table 1 Ionic conductivity of several solid electrolytes/S cm^{-1}

	PI-PEO	PI–$PEO_{0.8}$–$LATP_{0.2}$	PI–$PEO_{0.8}$–$(Al_2O_3)_{0.2}$	PI–$PEO_{0.2}$–PDA@$LATP_{0.8}$	PI–$PEO_{0.2}$–PDA@$(Al_2O_3)_{0.8}$
30 °C	7.94×10^{-6}	5.01×10^{-5}	1.03×10^{-5}	2.07×10^{-4}	2.94×10^{-5}
80 °C	3.18×10^{-4}	9.31×10^{-4}	5.24×10^{-4}	2.05×10^{-3}	5.57×10^{-4}

temperature so as to improve the ionic conductivity of the composite electrolyte is better than adding them at a high temperature, which can be attributed to the low crystallinity of PEO at a high temperature.

It can be concluded from the data in Table 1 that when inactive inorganic nanoparticles are added to PEO, the ionic conductivity of the composite electrolyte increases due to the decrease of the crystallinity of PEO; compared with adding inactive Al_2O_3 nanoparticles, adding the active ionic conductor LATP has a significantly better effect of improving the ionic conductivity, indicating that LATP plays an important role in ion conduction in the composite electrolyte system. When LATP is coated with PDA, the transport of Li^+ through the LATP crystal and the interface between crystals is not blocked. The ionic conductivity of PI–$PEO_{0.2}$–PDA@$LATP_{0.8}$ is one order of magnitude higher than that of PI–$PEO_{0.2}$–PDA@$(Al_2O_3)_{0.8}$. When the ratio of LATP to PEO is relatively low, the inorganic ionic conductors are not sufficient to form a continuous Li^+ channel in the composite electrolyte, so Li^+ conduction mainly depends on the PEO chain segments and PEO–LATP interface. When the proportion of LATP is high and evenly dispersed in PEO, Li^+ can conduct between continuous LATP phases in addition to conducting on the PEO chain segments and the PEO-LATP interface, resulting in additional lithium ion transmission channels and, thus, an improved ion conductivity.

3 Experimental

3.1 Materials

Ammonium dihydrogen phosphate ($NH_4H_2PO_4$, AR), lithium acetate dihydrate ($CH_3COOLi{\cdot}2H_2O$, AR), aluminum nitrate dihydrate (Al $(NO_3)_3{\cdot}9H_2O$, 99.99%), tetrabutyl titanate Yuanye biological company. *N*,*N*-Dimethylacetamide (DMAc, AR), *N*-methylpyrrolidone (NMP, AR), dimethyl carbonate (DMC, AR), vinyl carbonate (EC, AR) and acetonitrile (ACN, AR) are all products of Beijing Chemical Works. Al_2O_3 powder (150 nm, 99.9%) was purchased from Shanghai Aladdin Bio-Chem Technology Co. Ltd. PI nanofiber film was homemade according to the literature.[16] Polyethylene oxide (PEO, M_w = 600 000) and lithium trifluoromethylsulfonate amide (LiTFSI, 99.95%) were purchased from Sigma-Aldrich Company, USA. Polyvinylidene fluoride (PVDF, HSV900) is a product of the Arkema Company, France. Lithium chips, battery cases and accessories, and $LiNi_{0.8}Co_{0.1}Mn_{0.1}O_2$ were purchased from Shenzhen kejing Zhida Technology Co. Ltd.

3.2 Preparation of materials

3.2.1 LATP particles coated with polydopamine. LATP nanoparticles were prepared according to the method reported in the literature 16. The procedure of coating LATP with dopamine is as follows: 120 mg of dopamine hydrochloride (2 mg mL^{-1}) was dissolved in 60 mL of Tris–HCl solution (pH = 8.5). When the color of the solution began to darken, 5 g of LATP particles were added and sonicated for 10 min, followed by magnetic stirring for 12 h. Then, the obtained particles were washed with deionized water, filtered and dried under vacuum at 60 °C for 24 h to yield light brown PDA@LATP products.

3.2.2 Preparation of composite solid electrolyte and reference samples. Under the protection of Argon, PEO and LiTFSI were dissolved in acetonitrile at a molar ratio of PEO : Li = 8 : 1 to obtain a 10 wt% solution. The powder of PDA@LATP, four times the weight of PEO in quantity, was mixed with the above solution and magnetic stirred for 24 h to yield a suspension (PDA@LATP : PEO = 8 : 2), which was subsequently cast on an electrospun PI film using the method reported in the literature.[16] The PDA@LATP and PEO infiltrated into the interstices of the PI fibers to form a flexible composite film after curing. After vacuum drying at 50 °C for 48 h and hot pressing, a PI-PEO-PDA@LATP composite solid electrolyte with a thickness of 30 μm was obtained.

The PI-PEO-PDA@Al_2O_3 reference samples were prepared by replacing LATP with an equal quantity of nanoscale Al_2O_3 particles coated with PDA. ($C_{16}H_{36}O_4Ti$, AR), dopamine hydrochloride ($C_8H_{11}NO_2{\cdot}HCl$, 98%) are all products of Sinopharm Chemical Reagent Co., Ltd. Tris–HCl buffer solution (pH = 8.5) was produced by the Shanghai.

3.3 Characterization and tests

The micro morphology of the samples was observed by a scanning electron microscope (SEM, Hitachi S-4800, Japan) and a transmission electron microscope (TEM, Hitachi JEM-2100F, Japan). The particle size was measured by a Zeta potential nanoparticle Analyzer (Malvern Zetasizer Nano ZS, UK). The contact angle between the LATP electrolyte and PEO solution was measured by a Dataphysics OCA-20 Apparatus (Germany). The phase state of the samples was determined by an X-ray diffractometer (XRD, Bruker D8 focus, Germany).

The electrochemical stability window of the composite electrolyte assembled into "SS|electrolyte|Li" batteries was tested using linear sweep voltammetry (LSV, 2.5–6 V, 10 mV s^{-1}) of an

electrochemical workstation (Zahner Zennium, Germany). The "SS|electrolyte|SS" blocking batteries were tested by the AC impedance method (EIS, scanning range 0.1–10^6 Hz, amplitude 5 mV). The intersection of the measured AC impedance curve and the real axis is the bulk resistance R_b (Ω) of the separator. Ionic conductivity η (S cm^{-1}) was calculated according to the following formula: $\eta = d/(R_bS)$, wherein, d is the thickness of the electrolyte (cm), and S is the effective area of the electrolyte (cm^2).

A self-made apparatus was used to characterize the flexibility of the electrolyte according to the literature.[23] The equipment consisted of three devices: a STX trapezoidal screw linear slide, a stepping motor, and a controller. Two ends of the electrolyte film were fixed. During the test, the sliding table drove the sample film to reciprocate in a bending/stretching motion. A demo video of the test is available in the ESI.†

The cathode was produced by dispersing $LiNi_{0.8}Co_{0.1}Mn_{0.1}O_2$, Super-P, and PVDF evenly into NMP with a mass ratio of 84 : 10 : 6 to obtain a mixture with a solid content of 20%, which was stirred for 12 h to form a uniformly dispersed suspension. Then, the suspension was blade-coated onto an aluminum foil (16 μm). After drying (in an air dry oven for 5 h at 60 °C and in a vacuum oven for 12 h at 120 °C under −0.1 MPa) and a hot-pressing process (80 °C), a NCM811 cathode was obtained with a thickness of 90 μm and a mass loading of 9.1 mg cm^{-2}. With the NCM 811 cathode, PI-PEO-PDA@LATP electrolyte and lithium metal anode, 2032 batteries were assembled. In order to improve the interface performance of the solid electrolyte, 5 μL cm^{-2} of liquid electrolyte (1 M Li TFSI in DMC : EC = 1 : 1) was added onto the surface of lithium metal. All the batteries were assembled in a glove box and tested with a battery test system (CT2001A, Landian Co., Ltd, China).

4 Conclusions

We coated LATP nanoparticles with polydopamine, which reduced the surface energy of the particles, improved the affinity with PEO, and hence successfully dispersed a high proportion of LATP in PEO without aggregation. The flexible composite solid electrolyte PI–$PEO_{0.2}$–PDA@$LATP_{0.8}$ constructed by loading $PEO_{0.2}$–PAD@$LATP_{0.8}$ on electrospun PI films has an ionic conductivity of 2.07×10^{-4} at 30 °C and 2.05×10^{-3} S cm^{-1} at 80 °C, with an electrochemical stability window of 5.2 V.

In this electrolyte, Li^+ conduction mainly has three forms: conduction on the chain segment of the PEO amorphous region, conduction on the LATP–PEO interface, and conduction between the continuous LATP phases. The coating of LATP by PDA does not block the transport of Li^+ either inside the crystal or at the crystal interface. The NCM811‖Li quasi-solid state batteries assembled with PI–$PEO_{0.2}$–PDA@$LATP_{0.8}$ exhibit a good cycle performance: the initial discharge capacity at 30 °C is 178.0 mA h g^{-1}, with the remaining capacity after 200 cycles of 172.1 mA h g^{-1} (96.7%), and the discharge capacity at a 3C rate is 105.5 mA h g^{-1}, which is significantly superior to that of the PI–$PEO_{0.8}$–$LATP_{0.2}$ electrolyte. This is because, after being coated by PDA on their surface, the surface energy of the LATP nanoparticles is reduced, making the LATP particles evenly dispersed in PEO. Meanwhile, the higher LATP content is conducive to the construction of a continuous LATP ion transmission channels in the composite solid electrolyte, which has consequently improved the lithium ion conductivity.

Author contributions

Lei He: Investigation, data curation, writing – original draft. Jian-Hua Cao: investigation, writing – review & editing. Ya-Kun Wang: translation. Dayong Wu: writing – review & editing, funding acquisition.

Conflicts of interest

There are no conflicts to declare.

Acknowledgements

This work was financially supported by the National Key R&D Program "New Energy Vehicles" Pilot Project (2016YFB0100105). This paper was translated by Mrs Ya-Kun Wang.

References

1 P. Albertus, S. Babinec, S. Litzelman and A. Newman, Status and challenges in enabling the lithium metal electrode for high-energy and low-cost rechargeable batteries, *Nat. Energy*, 2017, **3**(1), 16–21.
2 W. Xu, J. Wang, F. Ding, X. Chen, E. Nasybulin, Y. Zhang and J. G. Zhang, Lithium metal anodes for rechargeable batteries, *Energy Environ. Sci.*, 2014, **7**(2), 513–537.
3 W. Liu, S. W. Lee, D. Lin, F. Shi, S. Wang, A. D. Sendek and Y. Cui, Enhancing ionic conductivity in composite polymer electrolytes with well-aligned ceramic nanowires, *Nat. Energy*, 2017, **2**(5), 17035.
4 Y. Li, W. Zhou, X. Chen, X. Lu, Z. Cui, S. Xin, L. Xue, Q. Jia and J. B. Goodenough, Mastering the interface for advanced all-solid-state lithium rechargeable batteries, *Proc. Natl. Acad. Sci. U. S. A.*, 2016, **113**(47), 13313–13317.
5 S. Choudhary and R. J. Sengwa, Effects of different inorganic nanoparticles on the structural, dielectric and ion transportation properties of polymers blend based nanocomposite solid polymer electrolytes, *Electrochim. Acta*, 2017, **247**, 924–941.
6 J. Pcharski, PEO based composite solid electrolyte containing Nasicon, *Solid State Ionics*, 1988, **28–30**, 979–982.
7 B. Chen, Z. Huang, X. Chen, Y. Zhao, Q. Xu, P. Long, S. Chen and X. Xu, A new composite solid electrolyte PEO/$Li_{10}GeP_2S_{12}$/SN for all-solid-state lithium battery, *Electrochim. Acta*, 2016, **210**, 905–914.

8 J. Zheng, M. Tang and Y. Y. Hu, Lithium ion pathway within $Li_7La_3Zr_2O_{12}$-polyethylene oxide composite electrolytes, *Angew. Chem., Int. Ed.*, 2016, **55**(40), 12538–12542.
9 B. Li, Q. Su, L. Yu, D. Wang, S. Ding, M. Zhang, G. Du and B. Xu, $Li_{0.35}La_{0.55}TiO_3$ nanofibers enhanced poly(vinylidene fluoride)-based composite polymer electrolytes for all-solid-state batteries, *ACS Appl. Mater. Interfaces*, 2009, **11**, 42206–42213.
10 L. Chen, Y. Li, S. P. Li, L. Z. Fan, C. W. Nan and J. B. Goodenough, PEO/garnet composite electrolytes for solid-state lithium batteries: from ''ceramic-in-polymer'' to ''polymer-in-ceramic'', *Nano Energy*, 2018, **46**, 176–184.
11 A. S. Pandian, X. C. Chen, J. Chen, B. S. Lokitz, R. E. Ruther, G. Yang, K. Lou, J. Nanda, F. M. Delnick and N. J. Dudney, Facile and scalable fabrication of polymer–ceramic composite electrolyte with high ceramic loadings, *J. Power Sources*, 2018, **390**, 153–164.
12 S. Kalnaus, A. S. Sabau, W. E. Tenhaeff, N. J. Dudney and C. Daniel, Design of composite polymer electrolytes for Li ion batteries based on mechanical stability criteria, *J. Power Sources*, 2012, **201**, 280–287.
13 F. Croce, S. Sacchetti and B. Scrosati, high-performance composite polymer electrolytes for lithium batteries, *J. Power Sources*, 2006, **161**(1), 560–564.
14 F. Croce, L. Persi, B. Scrosati, F. Serraino-Fiory, E. Plichta and M. A. Hendrickson, Role of the ceramic fillers in enhancing the transport properties of composite polymer electrolytes, *Electrochim. Acta*, 2001, **46**(16), 2457–2461.
15 W. Liu, N. Liu, J. Sun, P. C. Hsu, Y. Li, H. W. Lee and Y. Cui, Ionic conductivity enhancement of polymer electrolytes with ceramic nanowire fillers, *Nano Lett.*, 2015, **15**(4), 2740–2745.
16 L. He, W. H. Liang, J. H. Cao and D. Y. Wu, PI-LATP–PEO electrolyte with high safety performance in solid-state lithium metal batteries, *ACS Appl. Energy Mater.*, 2022, **5**(4), 5277–5286.
17 S. Hong, Y. S. Na, S. Choi, I. T. Song, W. Y. Kim and H. Lee, Non-Covalent Self-Assembly and Covalent Polymerization Co-Contribute to Polydopamine Formation, *Adv. Funct. Mater.*, 2012, **22**(22), 4711–4717.
18 H. Lee, S. M. Dellatore, W. M. Miller and P. B. Messersmith, Mussel-inspired surface chemistry for multifunctional coatings, *Science*, 2007, **318**(5849), 426–430.
19 A. T. Tran, F. Huet, K. Ngo and P. Rousseau, Influence on the electrolyte resistance of the contact angle of a bubble attached to a disk electrode, *J. Electroanal. Chem.*, 2015, **737**, 114–122.
20 X. Xu, Y. Liu, J. Y. Hwang, O. O. Kapitanova, Z. Song, Y. K. Sun, A. Matic and S. Xiong, Role of Li-Ion Depletion on Electrode Surface: Underlying Mechanism for Electrodeposition Behavior of Lithium Metal Anode, *Adv. Energy Mater.*, 2020, **10**, 2002390.
21 Y. Liu, X. Xu, O. O. Kapitanova, P. V. Evdokimov, Z. Song, A. Matic and S. Xiong, Electro-Chemo-Mechanical Modeling of Artificial Solid Electrolyte Interphase to Enable Uniform Electrodeposition of Lithium Metal Anodes, *Adv. Energy Mater.*, 2022, **12**, 2103589.
22 X. Xu, X. Jiao, O. O. Kapitanova, J. Wang, V. S. Volkov, Y. Liu and S. Xiong, Diffusion Limited Current Density: A Watershed in Electrodeposition of Lithium Metal Anode, *Adv. Energy Mater.*, 2022, **12**, 2200244.
23 B. R. Cai, J. H. Cao, W. H. Liang, L. Y. Yang, T. Liang and D. Y. Wu, Ultraviolet-cured Al_2O_3–polyethylene terephthalate/polyvinylidene fluoride composite separator with asymmetric design and its performance in lithium batteries, *ACS Appl. Energy Mater.*, 2021, **4**, 5293–5303.